Journal of Magnetic Resonance **140,** 179–188 (1999)
Article ID jmre.1999.1816, available online at http://www.idealibrary.com on IDEAL®

A Rigorous Evaluation of Spin-Hamiltonian Parameters and Linewidth from a Polycrystalline EPR Spectrum

Sushil K. Misra

Physics Department, Concordia University, 1455 de Maisonneuve Boulevard West, Montreal, Quebec H3G 1M8, Canada

Received January 19, 1999; revised May 11, 1999

Details are given of a procedure to evaluate the spin-Hamiltonian (SH) parameters and the linewidth from a polycrystalline EPR spectrum by using a least-squares fitting (LSF) technique in conjunction with numerical diagonalization of the SH matrix. The required resonance line positions are computed rather quickly using a homotopy technique, in which the position at an external magnetic field (B) orientation (θ, φ) is used as the initial value in a LSF procedure to estimate the position at an infinitesimally close B-orientation, ($\theta + \delta\theta$, $\varphi + \delta\varphi$). The resonance line positions are calculated successively in this procedure for all orientations of B over a grid of (θ, φ) values for the unit sphere. The eigenvectors of the SH matrix are used to calculate the intensities of the EPR lines exactly for each orientation of B. Details are given of how to compute rigorously the first and second derivatives of the χ^2-function with respect to the SH parameters and the linewidth using the eigenvalues and eigenvectors of the spin-Hamiltonian matrix for a polycrystalline spectrum required in the LSF procedure. It is explained how this technique is generalized to include two or more magnetically inequivalent paramagnetic species, as well as how it is used for the simulation of other EPR-related spectra. The procedure is illustrated by evaluation of the Mn^{2+} SH parameters and Lorentzian linewidth from the 249.9-GHz EPR spectrum of Mn(γ-picoline)$_4$I$_2$.

I. INTRODUCTION

It is of considerable interest to be able to accurately evaluate the spin-Hamiltonian (SH) parameters characterizing paramagnetic species from polycrystalline EPR spectra. The polycrystalline spectrum is the superposition of the monocrystalline spectra expected for uniform distribution of $\mathbf{B}(\theta, \varphi)$ with respect to the symmetry axis of the single crystal where one exists. For polycrystalline samples, it is possible to achieve a precision similar to that for single crystals by following the procedure described in this paper, using the least-squares (LSF) technique. In this procedure, a large number of resonance line positions, obtained for a uniform distribution of orientations of the external magnetic field (**B**) with respect to the single-crystal symmetry axis, are fitted simultaneously to improve significantly the precision in the estimated values of the SH parameters. The procedure has been made rigorous by using the eigenvalues and eigenvectors of the SH matrix to calculate the required first and second derivatives of the χ^2-function as described in (*1*).

For many molecules, such as metalloproteins (*2*), it is not possible to grow single crystals of sufficient size to enable them to be mounted with their axes oriented in chosen directions for angular variation of EPR spectrum for varying orientations of **B** with respect to the crystal symmetry axis in order to evaluate SH parameters accurately. Moreover, it is not always possible to rotate either the crystal or the magnetic field, for experimental reasons or because the orientations of the axes change when structural phase-transitions occur, and it is not possible to reorient the crystal inside the cryostat at low temperatures. It is then preferable to record a polycrystalline (powder) spectrum. The possibility of fitting a large number of EPR resonance line positions simultaneously is then excluded, since only one spectrum, insensitive to the orientation of the external magnetic field, is available for a polycrystalline sample.

So far, SH parameters have been estimated for the case of larger spins by the use of brute-force techniques, wherein a polycrystalline spectrum is simulated by arbitrarily adjusting the parameter values. The set of values that provides the most reasonable fit is then considered to be the set representing the best values of the SH parameters. Also, the intensities were calculated using the zero-order wavefunctions, insensitive to the orientation of **B**, and perturbation expressions were used for the eigenvalues which may not be quite precise when the orientation of **B** and of the symmetry axis of the single crystal deviate significantly from each other and the zero-field splitting (ZFS) parameter, D, is relatively large. Markham and Reed (*3*), Zhang and Buckmaster (*4*), and Coffino and Peisach (*5*) have discussed the computational strategies involved in the simulation of polycrystalline spectra, especially using the matrix diagonalization (*4*, *5*). Recently, the homotopy technique, together with the diagonalization of the SH matrix (referred to hereafter as the HTMD method), has been proposed for a fast simulation of an EPR polycrystalline spectrum (*6*).

It is desirable that the parameter values are estimated by the use of a mathematical criterion, in which all the SH parameters and linewidth values are varied simultaneously in a systematic manner, using a LSF technique. This paper provides the details of a LSF procedure which can be used to estimate SH param-

1090-7807/99 $30.00

eter values from a polycrystalline spectrum to estimate the first and second derivatives of the χ^2-function with respect to the SH parameters and the linewidth by an exploitation of the HTMD method. Section II describes briefly the details of how to simulate a polycrystalline spectrum by the HTMD technique, while Section III deals with the estimation of the parameters from a polycrystalline spectrum using the LSF technique, including the details of how to calculate the first and second derivatives of the χ^2-function with respect to the parameters. Since analytic expressions are not available for the eigenvalues and spectral intensities, this is accomplished by numerical techniques employing the eigenvalues and eigenvectors of the SH matrix. Specific details are provided here for the Gaussian and Lorentzian resonance lineshapes. The recommended procedure for the application of the LSF technique to estimate SH parameter and linewidth values is outlined in Section IV. Extension to the case of two magnetically inequivalent paramagnetic species is discussed in Section V. An illustrative example, involving the evaluation of Mn^{2+} parameter values from a 249.9-GHz EPR spectrum of polycrystalline $Mn(\gamma\text{-picoline})_4I_2$, is given in Section VI. Discussion and concluding remarks are given in Section VIII.

II. SIMULATION OF POLYCRYSTALLINE SPECTRUM BY THE USE OF HOMOTOPY

This section provides an overview of how to simulate an EPR polycrystalline spectrum using the HTMD technique. (Misra (*6*) has given complete details about this new technique.) This spectrum is the summation of single-crystal spectra computed for a large number of uniformly distributed orientations (θ, φ) of **B** over the unit sphere weighted by $\sin\theta d\theta d\varphi$ to take into account the distribution of those crystallites whose principal axes are oriented in the interval $(d\theta, d\varphi)$ with respect to (θ, φ). Moreover, a lineshape function, $F(B_{ri}, B)$, which could be Gaussian or Lorentzian, centered at the resonant magnetic field value $B_r(i, \theta_j, \varphi_j, \nu_c)$ for the transition $i' \leftrightarrow i''$ at $\mathbf{B}(\theta, \varphi)$ at the microwave resonance frequency ν_c is required. (Hereafter, B_{ri} stands for $B_r(i, \theta_j, \varphi_j, \nu_c)$.) More complicated lineshape functions are occasionally appropriate as per the sample. In addition, each transition line position must be weighted in proportion to its transition probability.

The simulated spectrum is given by

$$S(B, \nu_c) = \int_{\theta=0}^{\pi/2} \int_{\varphi=0}^{2\pi} \sum_i P(i, \theta, \varphi, \nu_c) \times F(B_{ri}, B) d(\cos\theta) d\varphi, \quad [2.1]$$

where $P(i, \theta, \varphi, \nu_c)$ is the transition probability for the ith transition, between the resonance eigenpair levels, i' and i'', at ν_c for $\mathbf{B}(\theta, \varphi)$.

The integral in Eq. [2.1] describing a polycrystalline spectrum can be divided up into discrete sums:

$$S(B_k, \nu_c) = C \sum_{i,\theta_j,\varphi_j} P(i, \theta_j, \varphi_j, \nu_c) F(B_{ri}, B_k) \sin\theta_j. \quad [2.2]$$

In Eq. [2.2], the values of θ_j are in the interval 0 to $\pi/2$, while those of φ_j are in 0 to 2π, using a uniform grid of (θ_j, φ_j) values, and $\sin\theta_j$ takes into account the assumed uniform distribution of the crystallites constituting the polycrystalline sample. The method for determining the (θ_j, φ_j) grid is given in (*6*). The summation over k takes into account the probability of the amplitude of absorption at the magnetic field value B_k due to the lineshape function $F(B_{ri}, B)$ for the ith transition for the **B**-field orientation (θ_j, φ_j). Further, it has been assumed that all spins are characterized by the same values of spin-Hamiltonian parameters, i.e., their magnetic tensors are the same except for the orientations of their principal axes due to the polycrystalline nature of the sample.

Transition probability, P(i, θ, φ, ν_c). The transition probability

$$P(i, \theta, \varphi, \nu_c) \propto |\langle\Phi_{i'}|(B_{1x}S_x + B_{1y}S_y + B_{1z}S_z)|\Phi_{i''}\rangle|^2, \quad [2.3]$$

where S_α and $B_{1\alpha}$; $(\alpha = x, y, z)$ represent the components of the electron spin operator, **S**, and the modulation magnetic field $\mathbf{B}_1$. $|\Phi_{i'}\rangle$ and $|\Phi_{i''}\rangle$ are the eigenvectors of the spin-Hamiltonian matrix, H, corresponding to the energy levels of the resonance eigenpair, $E_{i'}$ and $E_{i''}$, $[H|\Phi_k\rangle = E_k|\Phi_k\rangle$; $k = i', i'']$.

For numerical computational convenience, the right-hand side of Eq. [2.3] can be expressed as

$$\begin{aligned}|\langle\Phi_{i'}|B_{1x}S_x + B_{1y}S_y + B_{1z}S_z|\Phi_{i''}\rangle|^2 &= B_1^2[|\sum_{\alpha=x,y,z} a_\alpha \mathrm{Re\ Tr}\{S_\alpha(|\Phi_{i''}\rangle \otimes \langle\Phi_{i'}|)\}|^2 \\ &\quad + |\sum_{\alpha=x,y,z} a_\alpha \mathrm{Im\ Tr}\{S_\alpha(|\Phi_{i''}\rangle \otimes \langle\Phi_{i'}|)\}|^2], \quad [2.4]\end{aligned}$$

where Tr stands for the trace of a matrix, Re and Im represent the real and imaginary parts, respectively, $\otimes$ represents the outer product of matrices or vectors, and $a_x = \sin\theta\cos\varphi$, $a_y = \sin\theta\sin\varphi$, and $a_z = \cos\theta$. Further, the various traces in Eq. [2.3] are expressed in a convenient form as

$$\begin{aligned}&\mathrm{Re\ Tr}[S_x(|\Phi_{i''}\rangle \otimes \langle\Phi_{i'}|)] \\ &\quad = \sum_j (S_x)_{j,j+1}\{\mathrm{Re}(|\Phi_{i''}\rangle \otimes \langle\Phi_{i'}|)_{j+1,j} \\ &\qquad + \mathrm{Re}(|\Phi_{i''}\rangle \otimes \langle\Phi_{i'}|)_{j,j+1}\} \quad [2.5a]\end{aligned}$$

$$\text{Im Tr}[S_x(|\Phi_{i''}\rangle \otimes \langle\Phi_{i'}|)] = \sum_j (S_x)_{j,j+1}\{\text{Im}(|\Phi_{i''}\rangle \otimes \langle\Phi_{i'}|)_{j+1,j} + \text{Im}(|\Phi_{i''}\rangle \otimes \langle\Phi_{i'}|)_{j,j+1}\} \quad [2.5b]$$

$$\text{Re Tr}[S_y(|\Phi_{i''}\rangle \otimes \langle\Phi_{i'}|)] = -\sum_j \text{Im}(S_y)_{j,j+1}\{\text{Im}(|\Phi_{i''}\rangle \otimes \langle\Phi_{i'}|)_{j+1,j} - \text{Im}(|\Phi_{i''}\rangle \otimes \langle\Phi_{i'}|)_{j,j+1}\} \quad [2.5c]$$

$$\text{Im Tr}[S_y(|\Phi_{i''}\rangle \otimes \langle\Phi_{i'}|)] = \sum_j \text{Im}(S_y)_{j,j+1}\{\text{Re}(|\Phi_{i''}\rangle \otimes \langle\Phi_{i'}|)_{j+1,j} - \text{Re}(|\Phi_{i''}\rangle \otimes \langle\Phi_{i'}|)_{j,j+1}\} \quad [2.5d]$$

In writing [2.5a]–[2.5d] the facts: (i) the matrices for S_x and S_y are real and imaginary, respectively, and (ii) the only nonzero elements of these matrices are $\text{Re}(S_x)_{j,j+1} = \text{Re}(S_x)_{j+1,j}$ and $\text{Im}(S_y)_{j,j+1} = -\text{Im}(S_y)_{j+1,j}$ have been taken into account. Further simplification can be made by noting the following: $\text{Re}(|\Phi_{i''}\rangle \otimes \langle\Phi_{i'}|)_{jk} = \text{Re}|\Phi_{i''}\rangle_j\, \text{Re}|\Phi_{i'}\rangle_k + \text{Im}|\Phi_{i''}\rangle_j\text{Im}|\Phi_{i'}\rangle_k$, $\text{Im}(|\Phi_{i''}\rangle \otimes \langle\Phi_{i'}|)_{jk} = -\text{Re}|\Phi_{i''}\rangle_j\text{Im}|\Phi_{i'}\rangle_k + \text{Im}|\Phi_{i''}\rangle_j\text{Re}|\Phi_{i'}\rangle_k$, where $|\Phi_i\rangle_j$ stands for the jth element of the column vector $|\Phi{:}\rangle$, etc.

$$\text{Re Tr}[S_z(|\Phi_{i''}\rangle \otimes \langle\Phi_{i'}|)] = \sum_j (S_z)_{j,j}\{\text{Re}|\Phi_{i''}\rangle_j\text{Re}|\Phi_{i'}\rangle_j + \text{Im}|\Phi_{i''}\rangle_j\text{Im}|\Phi_{i'}\rangle_j\} \quad [2.5e]$$

$$\text{Im Tr}[(S_z)(|\Phi_{i''}\rangle \otimes \langle\Phi_{i'}|)] = \sum_j (S_z)_{j,j}\{-\text{Re}|\Phi_{i''}\rangle_j\text{Im}|\Phi_{i'}\rangle_j + \text{Im}|\Phi_{i''}\rangle_j\text{Re}|\Phi_{i'}\rangle\}. \quad [2.5f]$$

As for sums, they are over $j = -S, -(S-1), -(S-2), \ldots, (S-2), (S-1)$ in [2.5a]–[2.5d], while they are over $j = -S, -(S-1), \ldots, (S-1), S$ in [2.5e] and [2.5f].

Resonance eigenpairs. The same resonance eigenpair, consisting of energy levels characterized by the electronic magnetic quantum numbers M and $M-1$, which describe the eigenvectors of H_{Ze}, the Zeeman part of the SH, should be used to calculate the resonance fields corresponding to the allowed fine-structure transitions as the orientation (θ, φ) of **B** is changed incrementally to $(\theta + \delta\theta, \varphi + \delta\varphi)$ until the unit sphere is covered. This is accomplished by first diagonalizing the matrix for H_{Ze} with the eigenvalues arranged in either decreasing or increasing order of their values (M-order), then transforming the matrix of H_{ZFS}, the zero-field splitting part of the spin-Hamiltonian by the matrix V, formed by the eigenvectors of H_{Ze} as columns, corresponding to the eigenvalues of H_{Ze}, in either decreasing or increasing M-order. H_Z is diagonal in this representation, since the diagonal elements are the eigenvalues of H_{Ze}. The transformed SH matrix $H^T = V(H_{Ze} + H_{ZFS})V\dagger$, so obtained in the basis of the eigenvectors of H_{Ze}, is then diagonalized to find its eigenvalues and eigenvectors, this time without ordering the eigenvalues, using an appropriate subroutine. This ensures that the resonance eigenpair M, $M-1$ retains the same label during the homotopy procedure. Otherwise, it is frequently impossible to follow the same eigenpair for a given transition as the **B** orientation is changed, particularly when this orientation is more than $\pi/6$ radians away from the crystal principal axis. Alternatively, since the M, $M-1$ eigenpair is unequivocally identified when the perturbation expressions are used, and H_{Ze} is chosen as the zero-order term (*5–7*), one can make a correspondence between the eigenvalues of the full Hamiltonian $(H_{Ze} + H_{ZFS})$ as obtained by matrix diagonalization and those calculated by perturbation, in which case the label M is well defined. This is done by finding the closest perturbation eigenvalues to the eigenvalues calculated by matrix diagonalization, the two sets not being identically the same.

Lineshape function $F(B_{ri}, B_k)$. The spectrum is then calculated by performing the sum in Eq. [2.2] with $P(i, \theta_j, \varphi_j, \nu_c)$ centered at $B_r(i, \theta_j, \varphi_j, \nu_c)$ with the lineshape function $F(B_{ri}, B_k)$, extended over a magnetic-field interval $\pm\Delta B$, related to $\Delta B_{1/2}$ (full width at half maximum) characteristic of the lineshape. (For example, $\Delta B = \pm 10\Delta B_{1/2}$ for good precision for Lorentzian lineshape.) The two most common lineshapes are

(i) the Gaussian lineshape,

$$F_G(B_{ri}, B_k) = K_G\exp[-(B_k - B_{ri})^2/\sigma^2], \quad [2.6a]$$

where B_{ri} is the resonant field value for the ith transition, σ is the linewidth, and K_G $\{=(1/B_\Delta)(\ln 2/\pi)^{1/2}\}$ is the normalization constant for the lineshape (*9, 10*). Here, $B_\Delta = (\frac{1}{2})B_{1/2}$ is the half width at half maximum (HWHM); and

(ii) the Lorentzian lineshape,

$$F_L(B_{ri}, B_k) = K_L\Gamma[\Gamma^2 + (B_k - B_{ri})^2]^{-1}, \quad [2.6b]$$

where Γ is the Lorentzian linewidth (HWHM $= (3)^{1/2}\Delta B_{pp}/2$, where ΔB_{pp} is the peak-to-peak first-derivative linewidth (*9*)).

More complicated lineshapes appropriate to polycrystalline samples are discussed by Misra (*11*) and in the references therein.

Calculation of line positions using homotopy. In the homotopy procedure (*6*), the resonance line position at the orientation $(\theta + \delta\theta, \varphi + \delta\varphi)$ is calculated from the knowledge of the line position at the orientation (θ, φ), using the least-squares fitting technique and Taylor series expansion (*12*),

$$B_r(i,\ \theta + d\theta,\ \varphi + \Delta\varphi) = \text{iterative limit}\left[-\left(\frac{\partial^2 S'}{\partial B^2}\right)^{-1}_{B'} \left(\frac{\partial S'}{\partial B}\right)_{B'} \right], \qquad [2.7]$$

where

$$S' \equiv (|E_{i'} - E_{i''}| - h\nu_c)^2, \qquad [2.7a]$$

h is Planck's constant and $E_{i'}$, $E_{i''}$ are the energies of the levels (i', i'') of the resonance eigenpair, and the iteration starts with $B'_r = B_r(i, \theta, \varphi)$. For calculation purposes, the square bracket in Eq. [2.13] is (*11*)

$$-\left(\frac{\partial^2 S'}{\partial B^2}\right)^{-1}\left(\frac{\partial S'}{\partial B}\right) = -(|E_{i'} - E_{i''}| - h\nu_c) \times \text{sign}\,(E_{i'} - E_{i''})/\left(\frac{\partial E_{i'}}{\partial B} - \frac{\partial E_{i''}}{\partial B}\right). \qquad [2.8]$$

The required eigenvalues and eigenvectors of the spin-Hamiltonian matrix are computed by the use of the subroutine JACOBI, which diagonalizes real symmetric matrices and is particularly efficient when the off-diagonal elements in the SH matrix are infinitesimally small, as is naturally the case in homotopy (*6, 13*).

Calculation of first-derivative EPR spectrum. Most experimental EPR data are obtained as the first derivative of the absorbed microwave power as functions of the external magnetic field intensity. This is true when $B_{mod} \leq (1/2)B_{1/2}$, where B_{mod} is the amplitude of the modulation magnetic field. The simulated first-derivative spectrum is calculated by taking the derivative of $S(B, \nu_c)$ (see Eq. [2.2]) with respect to B, along with that of the lineshape. Specifically, for the Gaussian and Lorentzian lineshapes, given by Eqs. [2.6a] and [2.6b], one has, respectively, for the first derivative,

$$\partial F_G(B_{ri}, B_k)/\partial B_k = -2K_G(B_k - B_{ri}) \times \exp(-(B_k - B_{ri})^2/\sigma^2)/\sigma^2, \qquad [2.9a]$$

$$\partial F_L(B_{ri}, B_k)/\partial B_k = -2K_L\Gamma[\Gamma^2 + (B_k - B_{ri})^2]^{-2} \times (B_k - B_{ri}). \qquad [2.9b]$$

The simulated first-derivative absorption spectrum is expressed from Eq. [2.2] as

$$F_c(B_k, \nu_c) = \partial S(B_k, \nu_c)/\partial B_k = C \sum_{i,\theta_j,\varphi_j} P(i, \theta_j, \varphi_j) \times \partial F(\omega_i, B_r(i, \theta_j, \varphi_j, \nu_c), B_k)/\partial B_k \sin\theta_j. \qquad [2.10]$$

From Eq. [2.18], one has the following for the two lineshapes using Eqs. [2.9a] and [2.9b].

Gaussian lineshape.

$$F_c(B_k, \nu_c) = \sum_i N|\langle\Phi_{i'}|B_{1x}S_x + B_{1y}S_y + B_{1z}S_z|\Phi_{i''}\rangle|^2 \times \exp[-(B_k - B_{ri})^2/\sigma^2] \times (B_k - B_{ri})/\sigma^2, \qquad [2.11a]$$

Lorentzian lineshape.

$$F_c(B_k, \nu_c) = \sum_i N|\langle\Phi_{i'}|B_{1x}S_x + B_{1y}S_y + B_{1z}S_z|\Phi_{i''}\rangle|^2 \times (B_k - B_{ri})\Gamma[\Gamma^2 + (B_k - B_{ri})^2]^{-2}. \qquad [2.11b]$$

In Eqs. [2.11a] and [2.11b], the constant, N, may be appropriately chosen, e.g., $|F_c(B_k, \nu_c)|_{max} = 1$, where $|F_c(B_k, \nu_c)|_{max}$ is the largest magnitude of all the calculated values.

III. ESTIMATION OF SH PARAMETERS AND LINEWIDTH FROM A POLYCRYSTALLINE SPECTRUM AND CALCULATION OF FIRST AND SECOND DERIVATIVES OF THE χ^2-FUNCTION

For application of the LSF technique proposed here, the χ^2-function is defined as the sum of the weighted squares of the differences between the calculated and measured first-derivative absorption resonances at the magnetic field values B_k within the magnetic-field interval considered,

$$\chi^2 = \sum_k [F_c(B_k, \nu_c) - F_m(B_k, \nu_c)]^2/\sigma_k^2, \qquad [3.1]$$

where $F_c(B_k, \nu_c)$ and $F_m(B_k, \nu_c)$ are, respectively, the normalized calculated (Eq. [2.11a] or [2.11b]) and measured values of the first-derivative EPR resonance signal, and σ_k is the weight factor (related to standard deviation of the datum k). The measured/calculated values may be normalized in such a way that the maximum of each is equal to 1.

In the LSF technique, the vector $\mathbf{a}^m$, whose components are the values of the SH parameters and the linewidth corresponding to the absolute minimum of the χ^2-function, can be obtained from $\mathbf{a}^i$, the vector whose components are the initially chosen values of the SH parameters (see Appendix I) and the linewidth (*1*):

$$\mathbf{a}^m = \mathbf{a}^i - (\mathbf{D}''(\mathbf{a}^i))^{-1}\mathbf{D}'. \qquad [3.2]$$

In Eq. [3.3], $\mathbf{D}'$ is the column vector whose elements are the first derivatives of the χ^2-function with respect to the parameters evaluated at $\mathbf{a}^i$ and $\mathbf{D}''$ is the matrix whose elements are the second derivatives with respect to the parameters evaluated at $\mathbf{a}^m$:

$$\mathbf{D}'_m = \left(\frac{\partial \chi^2}{\partial \mathbf{a}_m}\right)_{\mathbf{a}^i} \quad [3.3a]$$

$$\mathbf{D}''_{nm} = \left(\frac{\partial^2 \chi^2}{\partial \mathbf{a}_n \partial \mathbf{a}_m}\right)_{\mathbf{a}^m}. \quad [3.3b]$$

Since $\mathbf{a}^m$ is not known initially, the elements of the matrix $\mathbf{D}''$ are, in practice, evaluated with respect to $\mathbf{a}^i$, referred to as $\mathbf{D}''(\mathbf{a}^i)$. A new set of parameters, denoted by the vector $\mathbf{a}^f$, which replaces the vector $\mathbf{a}^m$, given by Eq. [3.2], is then calculated,

$$\mathbf{a}^f = \mathbf{a}^i - (\mathbf{D}''(\mathbf{a}^i))^{-1}\mathbf{D}'. \quad [3.4]$$

$\mathbf{a}^f$ is calculated iteratively until a sufficiently small value of the χ^2-function, consistent with experimental errors, is obtained. The errors in the values of the parameters can be calculated statistically from the matrix elements of $\mathbf{D}''$ (see Appendix II).

Calculation of D′ and D″

Equations [3.3a] and [3.3b] yield

$$D'_m = 2\sum_k [F_c(B_k, \nu_c) - F_m(B_k, \nu_c)]\left(\frac{\partial F_c(B_k, \nu_c)}{\partial a_m}\right)/\sigma_k^2 \quad [3.5a]$$

$$D''_{nm} = 2\sum_k \left\{[F_c(B_k, \nu_c) - F_m(B_k, \nu_c)]\left(\frac{\partial^2 F_c(B_k, \nu_c)}{\partial a_\nu \partial a_m}\right) + \left(\frac{\partial F_c(B_k, \nu_c)}{\partial a_n}\right)\left(\frac{\partial F_c(B_k, \nu_c)}{\partial a_m}\right)\right\}/\sigma_k^2. \quad [3.5b]$$

The first and second derivatives of $F_c(B_k, \nu_c)$, given by Eqs. [2.11a] and [2.11b], with respect to the parameters appearing in Eqs. [3.5a] and [3.5b], are as follows.

a. Gaussian lineshape.

$$\frac{\partial F_c(B_k, \nu_c)}{\partial a_m} = \sum_i N|\langle\Phi_{i'}|B_{1x}S_x + B_{1y}S_y + B_{1z}S_z|\Phi_{i''}\rangle|^2 \exp[-(B_k - B_{ri})^2/\sigma^2]2 \times (B_k - B_{ri})\left\{\frac{\partial B_{ri}}{\partial a_m} + (B_k - B_{ri})\frac{\partial \sigma}{\partial a_m}/\sigma\right\}/\sigma^2. \quad [3.6a]$$

In Eq. [3.6a], $\partial\sigma/\partial a_m = 1/w_G$, for $a_m = w_G\sigma$, $=0$ otherwise.

From Eq. [3.6a] the second derivative of $F_c(B_{k'}\nu_c)$ is

$$\frac{\partial^2 F_c(B_k, \nu_c)}{\partial a_n \partial a_m} = \sum_i N|\langle\Phi_{i'}|B_{1x}S_x + B_{1y}S_y + B_{1z}S_z|\Phi_{i''}\rangle|^2 \times \exp[-(B_k - B_r)^2/\sigma^2] \times \left\{[2(B_k - B_{ri})/\sigma^2]\left\{\frac{\partial^2 B_{ri}}{\partial a_n \partial a_m} - \frac{\partial B_{ri}}{\partial a_n}\frac{\partial \sigma}{\partial a_m}/\sigma - (B_k - B_{ri})\frac{\partial \sigma}{\partial a_n}\frac{\partial \sigma}{\partial a_m}/\sigma^2\right\} - \left\{2\left(\frac{\partial B_{ri}}{\partial a_n} + 2(B_k - B_{ri})\frac{\partial \sigma}{\partial a_n}/\sigma\right) - [2(B_k - B_{ri})/\sigma]^2 \times \left[\frac{\partial B_{ri}}{\partial a_n} + (B_k - B_{ri})\frac{\partial \sigma}{\partial a_n}/\sigma\right]\right\} \times \left[\frac{\partial B_{ri}}{\partial a_m} + (B_k - B_{ri})\frac{\partial \sigma}{\partial a_m}/\sigma^2\right]/\sigma^2\right\}, \quad [3.6b]$$

where account has been taken of the fact that the second derivative of σ with respect to the parameters, a_n, is zero.

b. Lorentzian lineshape.

$$\frac{\partial F_c(B_k, \nu_c)}{\partial a_m} = \sum_i N|\langle\Phi_{i'}|B_{1x}S_x + B_{1y}S_y + B_{1z}S_z|\Phi_{i''}\rangle|^2 \times \frac{1}{[\Gamma^2 + (B_k - B_{ri})^2]^2}\left\{\frac{\partial \Gamma}{\partial a_m}(B_k - B_{ri}) - \Gamma\frac{\partial B_{ri}}{\partial a_m}\right\} + \Gamma(B_k - B_{ri}) \times \left\{\frac{\partial}{\partial a_m}(1/[\Gamma^2 + (B_k - B_{ri})^2]^2)\right\}, \quad [3.7a]$$

where

$$\left\{\frac{\partial}{\partial a_m}(1/[\Gamma^2 + (B_k - B_{ri})^2]^2)\right\} = \left(-4\left[\Gamma\frac{\partial \Gamma}{\partial a_m} - (B_k - B_{ri})\frac{\partial B_{ri}}{\partial a_m}\right] \div [\Gamma^2 + (B_k - B_{ri})^2]^3\right). \quad [3.7b]$$

In Eqs. [3.7a] and [3.7b], $\partial\Gamma/\partial a_m = 1/w_L$, for $a_m = w_L\Gamma$, $=0$ otherwise.

From Eq. [3.7a],

$$\frac{\partial^2 F_c(B_k,\ \nu_c)}{\partial a_n \partial a_m} = \sum_i N|\langle\Phi_{i'}|B_{1x}S_x + B_{1y}S_y + B_{1z}S_z|\Phi_{i''}\rangle|^2 \times \frac{\partial}{\partial a_n}(1/[\Gamma^2 + (B_k - B_{ri})^2]^2) \times \left\{\frac{\partial \Gamma}{\partial a_m}(B_k - B_{ri}) - \Gamma\frac{\partial B_{ri}}{\partial a_m}\right\} - (1/[\Gamma^2 + (B_k - B_{ri})^2]^2) \times \left\{\frac{\partial \Gamma}{\partial a_m}\frac{\partial B_{ri}}{\partial a_n} + \frac{\partial \Gamma}{\partial a_n}\frac{\partial B_{ri}}{\partial a_m} + \Gamma\frac{\partial^2 B_{ri}}{\partial a_n \partial a_m}\right\} + \left\{\frac{\partial \Gamma}{\partial a_n}(B_k - B_{ri}) - \Gamma\frac{\partial B_{ri}}{\partial a_n}\right\} \times \left\{\frac{\partial}{\partial a_m}(1/[\Gamma^2 + (B_k - B_{ri})^2])\right\} + \Gamma(B_k - B_{ri}) \times \left\{\frac{\partial^2}{\partial a_n \partial a_m}(1/[\Gamma^2 + (B_k - B_{ri})^2])\right\}, \quad [3.7c]$$

where, from Eq. [3.7b],

$$\frac{\partial^2}{\partial a_n \partial a_m}(1/[\Gamma^2 + (B_k - B_{ri})^2]) = -4\left[\frac{\partial \Gamma}{\partial a_n}\frac{\partial \Gamma}{\partial a_m} + \frac{\partial B_{ri}}{\partial a_n}\frac{\partial B_{ri}}{\partial a_m} - (B_k - B_{ri})\frac{\partial^2 B_{ri}}{\partial a_n \partial a_m}\right] - 12\left[\Gamma\frac{\partial \Gamma}{\partial a_m} - (B_k - B_{ri})\frac{\partial B_{ri}}{\partial a_m}\right] \times \frac{\partial}{\partial a_n}[\Gamma^2 + (B_k - B_{ri})^2]^2/[\Gamma^2 + (B_k - B_{ri})^2]. \quad [3.7d]$$

In expressing Eq. [3.7d], account has been taken of the fact that the second derivative of Γ with respect to the parameters, a_n, is zero.

It is shown in Appendix III that the derivatives of B_{ri} in Eqs. [3.6a], [3.6b], and [3.7a] are given by

$$\frac{\partial B_{ri}}{\partial a_m} = -\left(\frac{\partial E_{i'}}{\partial a_m} - \frac{\partial E_{i''}}{\partial a_m}\right)\Big/\left(\frac{\partial E_{i'}}{\partial B_{ri}} - \frac{\partial E_{i''}}{\partial B_{ri}}\right), \quad [3.8a]$$

and

$$\frac{\partial^2 B_{ri}}{\partial a_n \partial a_m} = \left\{-\left(\frac{\partial^2 E_{i'}}{\partial a_n \partial a_m} - \frac{\partial^2 E_{i''}}{\partial a_n \partial a_m}\right)\left(\frac{\partial E_{i'}}{\partial B_{ri}} - \frac{\partial E_{i''}}{\partial B_{ri}}\right) + \left(\frac{\partial^2 E_{i'}}{\partial a_n \partial B_{ri}} - \frac{\partial^2 E_{i''}}{\partial a_n \partial B_{ri}}\right)\right\}\Big/\left(\frac{\partial E_{i'}}{\partial B_{ri}} - \frac{\partial E_{i''}}{\partial B_{ri}}\right)^2. \quad [3.8b]$$

In Eq. [3.8b], the required second derivatives of the eigenvalues are given in (*1*),

$$\frac{\partial^2 E_i}{\partial a_n \partial a_m} = \sum_k{}' \left\langle \Phi_i \left| \frac{\partial H}{\partial a_m} \right| \Phi_k \right\rangle \left\langle \Phi_k \left| \frac{\partial H}{\partial a_n} \right| \Phi_i \right\rangle \Big/ (E_i - E_k) + \text{complex conjugate}, \quad [3.9]$$

where, as well as in [3.10], the prime over the summation sign indicates that the sum excludes the term with $k = i$, that is the summation is over all the eigenvalues (and eigenvectors) of the SH matrix, except for $k = i$. For numerical computational convenience, Eq. [3.9] is rewritten as

$$\frac{\partial^2 E_i}{\partial a_n \partial a_m} = \sum_k{}' \text{Tr}\left[\frac{\partial H}{\partial a_m}(|\Phi_k\rangle\langle\Phi_k|)\frac{\partial H}{\partial a_n}(|\Phi_i\rangle\langle\Phi_i|)\right] \div (E_i - E_k) + \text{complex conjugate}. \quad [3.10]$$

IV. OPTIMUM SH PARAMETERS AND LINEWIDTH ESTIMATION FROM A POLYCRYSTALLINE SPECTRUM USING THE LSF TECHNIQUE

The approach recommended for the evaluation of the SH parameters and linewidth using the LSF method in conjunction with the HTMD method follows.

(i) A set of initial values of SH parameters and linewidth, which may be obtained by an adjustment of parameters over appropriate ranges by simulation of a polycrystalline spectrum either by using perturbation expressions or by matrix diagonalization, is chosen.

(ii) The spectrum is simulated using these values and the HTMD method (*6*). The corresponding χ^2-value is calculated using Eq. [3.1].

(iii) The first and second derivatives of the χ^2-value are calculated with respect to the parameters using Eqs. [3.3] and [3.4].

(iv) New values of the SH parameters are then calculated with the LSF procedure using Eq. [3.5] and the derivatives obtained in step (iii).

(v) The χ^2-value is now recalculated. Convergence is achieved if this value is less than or equal to a predetermined value, $(\chi^2)_{\min}$, consistent with experimental uncertainties, and further iterations are not required. The SH parameter and

linewidth values obtained in step (iv) are then the final values. The corresponding errors of the values of the SH parameters and linewidth are calculated statistically from the first and second derivatives of the χ^2-value using the expressions given in Appendix I.

(vi) If the χ^2-value calculated in step (v) is larger than $(\chi^2)_{\min}$, then steps (i)–(v) are repeated using the SH parameter and linewidth values obtained in step (v). This procedure is repeated until $\chi^2 \leq (\chi^2)_{\min}$.

(vii) If convergence is not achieved in step (vi) or the χ^2-value in any iteration is greater than that obtained in the previous iteration, then either the initial values of the SH parameters and linewidth used in step (i) are changed or the binary-chop technique described in Appendix IV is then used.

V. EXTENSION TO THE CASE OF TWO MAGNETICALLY INEQUIVALENT SPECIES

The resulting spectrum is a superposition of the spectra corresponding to the two species with the weight factors proportional to the populations of the two species in the sample when two magnetically inequivalent species are present in a polycrystalline sample. Consequently, there are a total of $(n_1 + n_2 + 1)$ parameters to be fitted, where n_1 and n_2 are the number of parameters characterizing the two species, since each species is characterized by its own set of parameters, and the additional parameter gives the fraction (f) of one of the species. The resultant spectrum is expressed as

$$F_c(a_{1i}, a_{2j}, f) = fF_{c1}(a_{1i}) + (1 - f)F_{c2}(a_{2j}), \quad [5.1]$$

where $i = 1, 2, \ldots, n_1$, and $j = 1, 2, \ldots, n_2$.

The experimental spectrum can be fitted to the parameters, using the derivatives of F_c with respect to the parameters a_{1i}, a_{2j}, f. It follows from Eq. [5.1] that

$$\partial F_c/\partial a_{1i} = f\partial F_{c1}/\partial a_{1i}; \quad [5.2a]$$

$$\partial F_c/\partial a_{2j} = (1 - f)\partial F_{c2}/\partial a_{2j}; \quad [5.2b]$$

$$\partial F_c/\partial f = F_{c1} - F_{c2}. \quad [5.2c]$$

The derivatives given by Eqs. [5.2a] or [5.2b] can be calculated in the same way as for the case of one species, except for the introduction of the weighting factors of f and $(1 - f)$, respectively, for species 1 and 2. Using Eqs. [5.2a]–[5.2c] for the required derivatives, the values of the parameters a_{1i}, a_{2j}, and the fraction f can be evaluated by the LSF technique in conjunction with the HTMD method, using the approach outlined in Section IV for only one species.

The procedure for two species outlined here can be similarly extended to the case of the presence of more than two magnetically inequivalent species.

VI. ILLUSTRATIVE EXAMPLE

The LSF/HTMD technique will now be illustrated to estimate the SH parameters and linewidth from the 249.9-GHz EPR spectrum for the Mn(γ-picoline)$_4$I$_2$ polycrystalline sample. This spectrum is characterized by a rather large value of the zero-field splitting parameter, D. This spectrum was reported by Lynch *et al.* (*7*) when the magnetic field was over the interval 4.4–9.4 T. It exhibited only fine structure, without any hyperfine structure. They analyzed this spectrum using the single-crystal SH in spherical coordinates ($z = r\cos\theta$, $x = r\sin\theta\cos\varphi$, $y = r\sin\theta\sin\varphi$):

$$H = g\mu_B B(S_z\cos\theta + S_x\sin\theta\cos\varphi + S_y\sin\theta\sin\varphi) + D[S_z^2 - S(S+1)/3] + E(S_x^2 - S_y^2), \quad [6.1]$$

where μ_B is the Bohr magneton, D and E are the zero-field splitting parameters, and the (x, y, z) axes define the coordinate system used, with the z-axis being coincident with the c-symmetry axis. The fourth-order ZFS terms were not included in the SH, because their effect is negligible at 249.9 GHz.

The values of parameters were estimated by Lynch *et al.* (*7*) from the observed spectrum, using third-order perturbation expressions for the energy (*7, 8*) and the same zero-order relative intensity ($|\langle M, m|S_+ + S_-|M', m\rangle|^2$) (*7*) of the $\Delta M = \pm 1$ "allowed" fine-structure transitions, independent of the orientation of the external magnetic field with respect to the axis of the various crystallites constituting the polycrystalline spectrum. Guided by these, the following initial values of the parameters were used: $g = 2.000$, $D/g\mu_B = 1.07$ T, $E/g\mu_B = 10$ mT, $\Delta B_{pp} = 70$ mT. (ΔB_{pp} is related to the Lorentzian linewidth (Eq. [2.6b]): $\Delta B_{pp} = 2\Gamma/(3)^{1/2}$ (*9*)). These initial values, used in the LSF technique in conjunction with the HTMD method, lead to the values of the SH parameters and the linewidth: $g = 2.00218 \pm 0.00001$, $D/g\mu_B = 1.092 \pm 0.001$ T, $E/g\mu_B = -1.27 \pm 0.15$ mT, $\Delta B_{pp} = 67.92 \pm 0.05$ mT. Figure 1 shows the experimental spectrum, along with the spectrum simulated using these values.

In addition, successful application has been made of the LSF/HTMD method as proposed here to evaluate the Mn^{2+} parameters from 249.9- and 95-GHz data on tetrahedrally distorted compounds: dichloro-, dibromo-, diiodo-bis(triphenylphosphine) dioxide manganese complexes [14].

VII. COMPUTATIONAL TIME REQUIRED IN THE EVALUATION OF PARAMETERS BY THE HTMD/LSF PROCEDURE

A detailed discussion of computational times required in the simulation of a Mn^{2+} polycrystalline spectrum by the HTMD/LSF procedure has been provided in Ref. (*6*). It was 4 h 9 min 1.77 s on the IBM RS/6000 Unix computer at the Cornell University Theory Center (CUTC) for one simulation using a grid of 300 θ

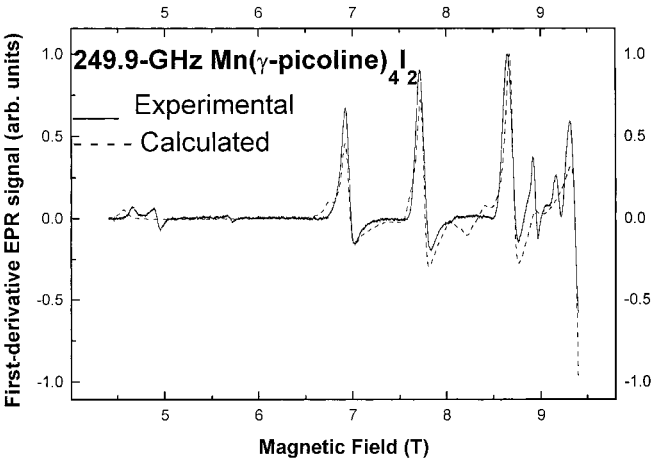

FIG. 1. EPR spectrum (249.9 GHz) for Mn^{2+} in polycrystalline Mn(γ-picoline)$_4I_2$ simulated by the HTMD technique using the SH parameter and linewidth values as obtained by the LSF technique: $g = 2.00218$, $D/g\mu_B = 1.092$ T, $E/g\mu_B = -1.27$ mT, $W = 67.92$ mT, and the observed experimental spectrum measured in the B-field interval 4.4–9.4 T. (The magnetic field could not exceed 9.4 T experimentally.) It is noted that the experimental peaks not corresponding to those in the simulated spectrum belong to an unidentified impurity (*7*).

values, 90 φ values per θ value. On the other hand, the time required for a simulation using third-order perturbation expressions was only 7 s! Since, in the LSF evaluation of parameters, one needs the first and second derivatives of the simulated spectrum with respect to the parameters, calculated using the same eigenvalues/eigenvectors as those required in the simulation, the computational time required for one iteration in the evaluation of parameters will be only somewhat longer than that required for simulation. Accordingly, it turned out to be, on the average, 5 h 0 min 53 s per iteration on the same CUTC computer for a grid consisting of 150 θ values (N.B., one-half of those used for simulation), 90 φ values per θ value, including a new simulation of the spectrum with the final values of the parameters. Of course, if more than one iteration is required to calculate the final set of parameters, the overall computational time will increase correspondingly. Finally, it is noted that computational time is no longer a barrier nowadays due to readily available inexpensive fast PC computers. Further, the number of iterations required is reduced if the initially chosen values of the parameters are close to those corresponding to the absolute minimum of the χ^2-value. Choice of initial values is explained, in particular, in Appendix I.

VIII. DISCUSSION AND CONCLUDING REMARKS

The method for evaluating the SH parameters and the linewidth from a CW EPR polycrystalline spectrum using the LSF procedure, in conjunction with the HTMD method which has been described here, is rigorous because it is not based on any approximations. The relative intensities have also been calculated using the exact eigenvectors, corresponding to the energy levels of the resonance eigenpairs. The first and second derivatives of the χ^2-function are calculated rigorously using numerical techniques based on the eigenvalues and eigenvectors of the SH matrix, for which the required expressions have here been listed explicitly for the Gaussian and Lorentzian lineshapes. The method has the advantage that it can be extended to include the presence of an arbitrary number of magnetically inequivalent species. In addition, it is relatively fast due to using the homotopy technique. (For an appreciation of computer times required, see Section VIII and (*6*).)

One example has been included here to illustrate the proposed procedure, and three examples will appear in a separate publication (*14*). Additional illustrative examples are not necessary, since as discussed in (*6*), the ability to calculate the EPR resonance angular variation (*1*) is sufficient to ensure the simulation of a polycrystalline spectrum, which is the weighted superposition of single-crystal spectra (*6*).

Although the procedure has been described for the "field-swept" EPR spectrum, it is equally applicable to "frequency-swept" spectrum, since the resonance condition, given by Eq. [II.1], still remains the same. As well, by modulating the external magnetic field, **B**, which remains constant, one records the first derivative of the lineshape as discussed here for the field-swept case.

The procedure outlined in this paper can be easily extended to evaluate the parameters describing electron-nuclear double resonance (ENDOR), solid-state nuclear magnetic resonance (NMR), nuclear quadrupole resonance (NQR), and electron spin-echo (ESE) envelope modulation spectra from polycrystalline samples, as well as to include hyperfine structure (*15, 16*).

It is hoped that the procedure outlined in this paper will be useful for where single-crystal samples are not available, e.g., metalloproteins (*2*), or when it is experimentally difficult to rotate single crystals and/or record more than one EPR spectrum at liquid-helium temperatures, or below a phase-transition temperature when the magnetic-axes orientations are not known. Further, it is noted that the availability of high-speed personal computers means that the simulation of a polycrystalline EPR spectrum does not require access to large computational facilities.

APPENDIX I

Choice of Initial Values Required in the LSF Procedure

For achieving convergence in the LSF procedure, it is necessary that the initial values chosen are reasonably close to those corresponding to the absolute minimum of the χ^2-value, represented by the components of the vector $\mathbf{a}^m$ in Section III. The procedure will not converge if they are far removed from $\mathbf{a}^m$. To this end, it is helpful to study the features of the experimental spectrum, i.e., the peaks, and to simulate the EPR spectrum with trial values using perturbation expressions, for which one needs negligible computational time as discussed in Section VII. One can estimate the values of the large ZFS parameters D and E from the

TABLE 1

Positions of Peaks for Polycrystalline Mn^{2+} ($g = 2$) Spectrum for η ($=D/E$) = 0 (Axial Symmetry) and η = 1/3 (Maximum Orthorhombic Distortion) (*7*)

Position of peak ($B_0 = h\nu/g\mu_B$, $D_0 = D/g\mu_B$)	Transition or turning point	
	($\eta = 0$)	($\eta = 1/3$)
$B_0 - 4D_0$	$5/2 \leftrightarrow 3/2$ (z)	$5/2 \leftrightarrow 3/2$ (z) $-3/2 \leftrightarrow -5/2$ (y)
$B_0 - 2D_0$	$3/2 \leftrightarrow 1/2$ (z) $-3/2 \leftrightarrow -5/2$ (x, y)	$3/2 \leftrightarrow 1/2$ (z) $-1/2 \leftrightarrow -3/2$ (y)
$B_0 - D_0$	$-1/2 \leftrightarrow -3/2$ (x, y)	
B_0	$1/2 \leftrightarrow -1/2$ (x, y, z) (for splitting due to higher order terms, see Note)	$5/2 \leftrightarrow 3/2$ (x) $3/2 \leftrightarrow 1/2$ (x) $1/2 \leftrightarrow -1/2$ (x, y, z) $-1/2 \leftrightarrow -3/2$ (x) $-3/2 \leftrightarrow -5/2$ (x)
$B_0 + D_0$	$3/2 \leftrightarrow 1/2$ (x, y)	
$B_0 + 2D_0$	$-1/2 \leftrightarrow -3/2$ (z) $5/2 \leftrightarrow 3/2$ (x, y)	$-1/2 \leftrightarrow -3/2$($z$) $3/2 \leftrightarrow 1/2$ (y)
$B_0 + 4D_0$	$-3/2 \leftrightarrow -5/2$ (z)	$-3/2 \leftrightarrow -5/2$ (z) $5/2 \leftrightarrow 3/2$ (y)

Note. The letters x, y, and z represent the orientation of the external Zeeman field with respect to the ZFS tensor axis. It is noted that higher order terms break the symmetry of the spectrum and cause a large splitting in the $1/2 \leftrightarrow -1/2$ transition into three turning points: 0° (z) and 90° (x, y) transitions, along with a line at 41.8° for $\eta = 0$. The rhombic distortion, η, splits some lines. The positions of the 0° or z transitions are insensitive to η. But the $\pm D$ lines for axial symmetry, being in-plane transitions, are very sensitive to rhombic distortion. These lines move as η increases and are completely lost at full rhombic distortion. The B_0 region at full rhombic distortion maybe characterized by a single line or a complex pattern of many lines depending on the value of D and linewidth. The positions of the peaks for the intermediate values $0 < \eta < 1/3$ can be obtained by extrapolation.

positions of the peaks. Basically, as discussed in Ref. (*7*) in context with the Mn^{2+} ion, the rhombic distortion ($\eta = D/E$) and the value of D can be estimated from the peak positions. The positions of the peaks expected for the two extreme cases are given in Table 1: $\eta = 0$ (axial symmetry) and $\eta = 1/3$ (maximum rhombic distortion). As for intermediate cases, one can make an educated guess by extrapolation between these two cases.

APPENDIX II

Expressions for Statistical Errors of Parameters

As discussed in (*17*), the errors Δa_j in the parameters, as evaluated by the LSF method, can be calculated statistically from the matrix $\mathbf{D}''$ formed by the matrix elements which are the second derivatives of the χ^2-function with respect to the parameters as given by Eq. [3.3b]. It is important to take into account appropriately the weight factors, σ_k, for the data points appearing in the expression for the χ^2-function, Eq. [3.1], which depend upon the experimental uncertainties. Finally,

$$\Delta a_j = (\epsilon_{jj})^{1/2}, \tag{I.1}$$

where ϵ_{jj} are the diagonal elements of the matrix $\boldsymbol{\epsilon}$:

$$\boldsymbol{\epsilon} = (\tfrac{1}{2}\mathbf{D}'')^{-1}. \tag{I.2}$$

It is noted that the nondiagonal elements, ϵ_{jk} ($j \neq k$), represent the correlations among the errors of the various parameters (*17*).

APPENDIX III

Calculation of Derivative of B_{ri} with Respect to the Parameters and Linewidth

If one starts with the resonance condition for the transition $i' \leftrightarrow i''$ which occurs at the field B_{ri},

$$h\nu = E_{i'} - E_{i''}. \tag{II.1}$$

Then, taking the derivative of Eq. [II.1] with respect to the parameter a_m and taking explicit account of the dependence of $E_{i'}$, $E_{i''}$ on a_m and B_{ri}, and of implicit dependence of B_{ri} on a_m, yields

$$\frac{\partial B_{ri}}{\partial a_m} = -\left(\frac{\partial E_{i'}}{\partial a_m} - \frac{\partial E_{i''}}{\partial a_m}\right) \Big/ \left(\frac{\partial E_{i'}}{\partial B_{ri}} - \frac{\partial E_{i''}}{\partial B_{ri}}\right). \tag{II.2}$$

The derivative of Eq. [II.2] with respect to a_n yields Eq. [3.8b].

Using Feynman's theorem (*1*), the derivatives of the eigenvalues with respect to the parameters a_m and B_{ri} are

$$\frac{\partial E_{i'}}{\partial a_m} = \left\langle \Phi_{i'} \middle| \frac{\partial H}{\partial a_m} \middle| \Phi_{i'} \right\rangle \tag{II.3}$$

and

$$\frac{\partial E_{i'}}{\partial B_{ri}} = \left\langle \Phi_{i'} \middle| \frac{\partial H}{\partial B} \middle| \Phi_{i'} \right\rangle_{B=B_{ri}}. \tag{II.4}$$

In Eq. [II.3], $\partial H/\partial a_m$ is the spin operator whose coefficient is a_m in the SH given in Eq. [6.1]:

$$\frac{\partial H}{\partial g} = \mu_B B(S_z \cos\theta + S_x \sin\theta \cos\varphi + S_y \sin\theta \sin\varphi), \tag{II.5}$$

$$\frac{\partial H}{\partial D} = [S_z^2 - S(S+1)/3], \tag{II.6}$$

$$\frac{\partial H}{\partial E} = (S_x^2 - S_y^2), \tag{II.7}$$

while

$$\frac{\partial H}{\partial B} = g\mu_B(\cos\theta S_z + \sin\theta\cos\varphi S_x + \sin\theta\sin\varphi S_y), \quad \text{[II.8]}$$

where (θ, φ) is the orientation of **B** with respect to the z-axis.

APPENDIX IV

Binary-chop Technique to Achieve Convergence

When the initial values of the set of parameters chosen for an iteration, to be used in Eq. [3.2], are far from the absolute minimum of the χ^2-value, the resulting value of parameters may yield a χ^2-value which is greater than that obtained in the previous iteration being corrected to a local minimum. One may then invoke the binary-chop technique (*1*), in which the LSF correction in $\mathbf{a}^i$ to calculate $\mathbf{a}^f$ is reduced by a factor of 2 in Eq. [3.4], i.e., it is now $-(\mathbf{D}''(\mathbf{a}^i))^{-1}\mathbf{D}'/2$. If the resulting χ^2-value is still greater than that obtained in the previous iteration, this difference is again chopped by 2, and so on, until the resulting χ^2-value is less than that in the previous iteration. Finally, it is noted that the binary-chop technique may not always work if the initial values chosen are far apart from those corresponding to the absolute minimum of the χ^2-function. In that case, one has to reexamine the choice of initial values.

ACKNOWLEDGMENTS

The author is grateful to the Natural Sciences and Engineering Research Council of Canada for partial financial support (Grant OGP0004485) and to Dr. S. Isber for assistance in preparing the manuscript. He is particularly indebted to Professor Jack Freed of Cornell University, Ithaca, for encouraging him to develop a computer diagonalization procedure to simulate and fit powder spectra and to provide him with the opportunity to visit his laboratory for 3 months during his sabbatical leave, as well as continued use of his workstation "Skeeve" and Cornell University's IBM RS/6000 computer at the Theory Center. Thanks are due to Dr. B. Lynch for providing the experimental spectrum exhibited in Fig. 1 used here for the evaluation of the parameters by the LSF technique and helpful discussions on simulation procedure and to Professor Harvey Buckmaster for many helpful comments on the manuscript.

REFERENCES

1. S. K. Misra, *J. Magn. Reson.* **23,** 403 (1976).
2. References on metalloproteins are B. Chiswell, E. D. McKenzie, and L. F. Lindboy, *in* "Comprehensive Coordination Chemistry" (G. Wilkinson, R. D. Gillard, and J. A. McCleverty, Eds.), Vol. 4, pp. 1–122, Pergamon, Oxford (1987). For EPR crystallography of metalloproteins, see J. C. W. Chien and L. C. Dickinson, *in* "Biological Magnetic Resonance" (L. J. Berliner and J. Reuben, Eds.), Vol. 3, pp. 155–210, Plenum, New York (1981); for ESR of Iron Proteins, see T. D. Smith and J. R. Pilbrow, *in* "Biological Magnetic Resonance" (L. J. Berliner and J. Reuben, Eds.), Vol. 2, pp. 85–183, Plenum, New York (1980); for X- and Q-band EPR study of Cu^{2+}, VO^{2+}, and Gd^{3+} ions in bovine α-lactalbumin complexes, see G. Musci, G. H. Reed, and L. Berliner, *J. Inorg. Biochem.* **26,** 229 (1986); J. F. Boas, Electron paramagnetic resonance of copper proteins, *in* "Copper Proteins and Copper Enzymes" (R. Lontie, Ed.), Vol. 1, p. 6, CRC Press, Boca Raton, FL (1984). Additional references on metalloproteins are H. Beinert, Electron paramagnetic resonance in biochemistry: Past, present and future, *Biochem. Soc. Trans.* **13,** 542 (1985); G. Palmer, The electron paramagnetic resonance of metalloproteins, *Biochem. Soc. Trans.* **13,** 548 (1985); G. R. Hanson and J. R. Pilbrow, Metalloproteins, *in* "Electron Spin Resonance" (M. C. R. Symons, Ed.), Vol. 10B, p. 93, The Royal Society of Chemistry, London (1987); W. E. Blumberg and J. Peisach, Paramagnetic resonance studies of copper proteins, *Life Chem. Rep.* **5,** 5 (1987); G. R. Hanson and G. L. Wilson, Metalloproteins, *Electron Spin Reson.* **11B,** 209 (1988); J. J. Villafranca and F. M. Raushel, NMR and EPR investigations of bimetalloenzymes, *Adv. Bio-Inorg. Chem.* **4,** 289 (1990).
3. G. H. Reed and G. D. Markham, *in* "Biological Magnetic Resonance" (L. J. Berliner and J. Reuben, Eds.), Vol. 6, pp. 73–142, Plenum, New York (1984).
4. Y. P. Zhang and H. A. Buckmaster, *J. Magn. Reson.* **99,** 533 (1992); *ibid, J. Magn. Reson. A* **102,** 151 (1993); *ibid, J. Magn. Reson. A* **109,** 241 (1994).
5. A. R. Coffino and J. Peisach, *J. Magn. Reson. B* **111,** 127 (1996).
6. S. K. Misra, *J. Magn. Reson.* **137,** 83 (1999).
7. W. B. Lynch, R. S. Boorse, and J. H. Freed, *J. Am. Chem. Soc.* **115,** 10909 (1993).
8. S. K. Misra, *Physica B* **240,** 183 (1997).
9. C. P. Poole, Jr., "Electron Spin Resonance: A Comprehensive Treatise on Experimental Techniques," 1st ed., p. 776, Wiley–Interscience, New York (1967).
10. H. A. Buckmaster and J. C. Dering, *J. Appl. Phys.* **39,** 4486 (1968).
11. S. K. Misra, *Appl. Magn. Reson.* **10,** 193 (1996).
12. S. K. Misra and V. Vasilopoulos, *J. Phys. C Condens. Matter* **13,** 1083 (1980).
13. W. H. Press, S. A. Teukolsky, W. T. Vetterling, and B. P. Flannery, "Numerical Recipes in Fortran," 2nd ed., pp. 456–462, (Cambridge, Cambridge Univ. Press (1992). The details of JACOBI subroutine, which diagnalizes a $n \times n$ real symmetric, are described. The technique of using a real symmetric matrix to find the eigenvalues and eigenvectors of a complex Hermitian matrix, $\mathbf{A} + i\mathbf{B}$, by constructing a $2n \times 2n$ symmetric matrix using the real and imaginary parts of the SH matrix, $\begin{pmatrix} \mathbf{A} & -\mathbf{B} \\ \mathbf{B} & \mathbf{A} \end{pmatrix}$, is described on p. 475 [see also S. K. Misra, *Magn. Reson. Rev.* **10,** 285 (1986)]. [The eigenvalues of the $2n \times 2n$ matrix are degenerate in n pairs; each pair has the eigenvalues of the matrix $\mathbf{A} + i\mathbf{B}$, and the eigenvectors (in columns with $2n$ elements) corresponding to any pair are such that the sets of upper and lower n elements can be chosen to be, respectively, the real and imaginary parts of the corresponding eigenvalue of the matrix $\mathbf{A} + i\mathbf{B}$, such that $(\mathbf{A} + i\mathbf{B})(\mathbf{u} + i\mathbf{v}) = \lambda(\mathbf{u} + i\mathbf{v})$ leads to $\begin{pmatrix} \mathbf{A} & -\mathbf{B} \\ \mathbf{B} & \mathbf{A} \end{pmatrix}\begin{pmatrix} \mathbf{u} \\ \mathbf{v} \end{pmatrix} = \lambda\begin{pmatrix} \mathbf{u} \\ \mathbf{v} \end{pmatrix}$ and $\begin{pmatrix} \mathbf{A} & -\mathbf{B} \\ \mathbf{B} & \mathbf{A} \end{pmatrix} \times \begin{pmatrix} -\mathbf{v} \\ \mathbf{u} \end{pmatrix} = \lambda\begin{pmatrix} -\mathbf{v} \\ \mathbf{u} \end{pmatrix}$]. It is noted that the algorithm for the JACOBI subroutine given by Press *et al.* is erroneous. The correct JACOBI subroutine is available on the website http://netlib2.cs.utk.edu/.
14. R. M. Wood, D. M. Stucker, W. Bryan Lynch, S. K. Misra, and J. H. Freed, to be published.
15. S. K. Misra, *Magn. Reson. Rev.* **10,** 285 (1986).
16. To take into account hyperfine structure, i.e., electron-nuclear spin-coupled systems, in the evaluation of parameters from single-crystal EPR spectra using the LSF technique see S. K. Misra, *Phys. B* **121,** 193 (1983).
17. S. K. Misra and S. Subramanian, *J. Phys. C: Condens. Matter* **15,** 7199 (1982).